

EFFECTS OF THE MUON $g - 2$ ANOMALY ON DARK MATTER AND ACCELERATOR PHYSICS

R. Arnowitt, B. Dutta , B. Hu, and Y. Santoso

*Center For Theoretical Physics, Department of Physics, Texas A&M University,
College Station, TX 77843-4242, USA*

Abstract

The effect of the recently observed 2.6σ deviation of the muon anomalous magnetic moment ($a_\mu = (g_\mu - 2)/2$) from its Standard Model prediction is examined within the framework of supergravity models with grand unification and R parity invariance. The constraints of the Higgs mass bounds, the $b \rightarrow s\gamma$ bounds (including the large $\tan\beta$ NLO corrections) and the cosmological relic density of light neutralinos (including all slepton neutralino coannihilation effects) are included in the analysis. For universal soft breaking, the Higgs and $b \rightarrow s\gamma$ bounds puts a lower bound $m_{1/2} \gtrsim 300$ GeV, most of the parameter space now falling in the co-annihilation region. The 2σ lower bound on the magnetic moment anomaly places an upper bound of $m_{1/2} \lesssim 800$ GeV. It is seen that mSUGRA requires that $a_\mu \lesssim 50 \times 10^{-10}$. One finds for $m_h > 114$ GeV, that $\tan\beta > 5(7)$ for $A_0 = 0(-4m_{1/2})$ and for $m_h > 120$ GeV, one has $\tan\beta > 15(10)$ for $A_0 = 0(-4m_{1/2})$. The sparticle spectrum is now much constrained, and the reaches of the Tevatron RUN II, NLC, and LHC for new physics discovery are discussed. Dark matter detection rates are examined, and it is seen that future detectors now would be able to scan most of the parameter space. Models with non-universal soft breaking in the Higgs and third generation of squarks and sleptons are examined, and it is seen that a new Z s-channel annihilation of neutralinos in the early universe is possible with dark matter detection rates accessible to the next round of detectors.

1 Introduction

Recently, the Brookhaven E821 experiment has measured the muon anomalous magnetic moment, $a_\mu = (g_\mu - 2)/2$ for the μ^+ to remarkable accuracy ¹⁾:

$$a_\mu = 11659202(14)(6) \times 10^{-10} \quad (1)$$

This had led to a 2.6σ deviation from the prediction of the Standard Model (SM):

$$a_\mu^{\text{exp}} - a_\mu^{\text{SM}} = 43(16) \times 10^{-10} \quad (2)$$

Eq. (1) arises from an analysis of only about one quarter of the existing μ^+ data. Further, the 2001 run for the μ^- should result in about three times as much data as has been analysed for the μ^+ ²⁾. Thus the statistical error in the measurement should decrease by about a factor of 2.5. In addition, the theoretical error in the hadronic vacuum polarization contribution should also be reduced (perhaps by a factor of 2) by the analysis of the Novosibirsk, DAPHNE and Beijing data. (For an analysis of the current theoretical accuracy of the hadronic vacuum polarization contribution see ³⁾, and for an alternate view see ⁴⁾.) Thus by the beginning of 2002 it should be possible to know whether the anomaly in the muon magnetic moment of Eq. (2) is real. If it is indeed real it would imply the discovery of new physics. Because of the importance of this possibility, we will here assume that the anomaly is real, and analyze some of its consequences.

Supersymmetry offers a possible explanation of a deviation of a_μ from its SM value, and initial calculations of a_μ were made in the early 1980's using global supersymmetry ⁵⁾. However, in unbroken global supersymmetry there is a theorem that the total value of a_μ should vanish ⁶⁾, i.e.

$$a_\mu^{\text{SM}} + a_\mu^{\text{SUSY}} = 0 \quad (3)$$

Thus one needs broken supersymmetry to get a non-zero result, and how to do this in a phenomenologically acceptable way within the framework of global supersymmetry was problematical. The advent of supergravity (SUGRA), where acceptable spontaneous breaking of supersymmetry occurs, led to the SUGRA grand unified (GUT) models ⁷⁾. The first (partial) calculation of a_μ^{SUGRA} was done in ⁸⁾, and the first complete calculation in ⁹⁾. In the SUGRA GUT models, SUSY breaking at the GUT scale M_G , triggers the breaking of $SU(2) \times U(1)$ at the electroweak scale M_{EW} , and hence the SUSY mass scale M_{SUSY} obeys

$$M_{\text{SUSY}} \cong M_{\text{EW}} \cong \langle H \rangle \quad (4)$$

setting the scale of the SUSY masses to be in the 100 GeV - 1 TeV range, a range also needed to avoid the hierarchy problem. This mass scale was further supported by the fact that the LEP data is consistent with grand unification if the SUSY masses lie in the range ~ 100 GeV - 1 TeV. Further, SUGRA models with R parity invariance have a dark matter candidate, the lightest neutralino, $\tilde{\chi}_1^0$, with the astronomically observed amount of relic density when the SUSY masses are in this range. Thus with the mass range implied by the SUGRA GUT models, it was possible to predict roughly the size of a_μ^{SUGRA} , and in fact in ⁹⁾ it was argued that a_μ^{SUGRA} should become observable when the experiments had a sensitivity of about 20×10^{-10} , as is the case for Eq. (2).

We consider here, then the effect of a_μ^{SUGRA} for SUGRA GUT models possessing R parity invariance. In particular, we consider (1) the mSUGRA model ⁷⁾ with universal soft breaking at M_G , and (2) models with non-universal scalar masses at M_G for the Higgs bosons and the third generation of squarks and sleptons.

2 Calculational Details

In the following we impose the current experimental bounds on the SUSY parameter space and list now the important ones:

1. Accelerator bounds: (i) We consider two possible values for the light Higgs mass $m_h > 114$ GeV and $m_h > 120$ GeV. The first is the current LEP bound ¹⁰⁾ while the second represents a bound that the Tevatron Run IIB could achieve, if it does not discover the Higgs boson. (ii). We assume for the $b \rightarrow s\gamma$ branching ratio the roughly 2σ range:

$$1.8 \times 10^{-4} < BR(b \rightarrow s\gamma) < 4.5 \times 10^{-4} \quad (5)$$

2. Relic density bounds for the lightest neutralino. We chose here the range

$$0.025 \leq \Omega_{\tilde{\chi}_1^0} h^2 < 0.25 \quad (6)$$

where $\Omega_{\tilde{\chi}_1^0} = \rho_{\tilde{\chi}_1^0}/\rho_c$, and ρ_c is the critical density to close the universe: $\rho_c = 3H_0^2/8\pi G_N$ (and H_0 is the Hubble constant, $H_0 = h$ 100 km/sec Mpc, G_N the Newton constant). The lower bound in Eq. (6) is smaller than the conventional value of ~ 0.1 , but can take into account the possibility that there is more than one species of dark matter. Our results here, however, are insensitive to this lower bound and would not change significantly if it were raised to 0.05 or 0.1.

3. We use a 2σ bound on the muon magnetic moment anomaly of Eq. (2):

$$11 \times 10^{-10} < a_\mu^{\text{SUGRA}} < 75 \times 10^{-10} \quad (7)$$

As we will see these will combine to put strong constraints on the SUSY parameter space and allow us to greatly strengthen the predictions for the neutralino-proton dark matter cross sections $\sigma_{\tilde{\chi}_1^0-p}$, as well as determine what parts of the SUSY mass spectrum can be seen at the Tevatron Run II, LHC and NLC accelerators.

In order to get accurate results, it is necessary to include a number of corrections in the calculation, and we mention here the most important ones: (1) The allowed SUSY parameter space is now quite sensitive to the Higgs mass, and so an accurate calculation of m_h is important. We include here the one and two loop corrections¹¹⁾ and the pole mass corrections. The theoretical value of m_h is still uncertain by about 3 GeV, and so the experimental bound of $m_h > 114$ GeV will (conservatively) be interpreted as a theoretical evaluation of $m_h > 111$ GeV (and similarly $m_h > 120$ GeV as $m_h > 117$ GeV). (2) Large $\tan\beta$ NLO corrections to the $b \rightarrow s\gamma$ decay rate¹²⁾ are included. (3) Loop corrections to m_b and m_τ are included (which are important for large $\tan\beta$). (4) QCD renormalization group corrections in going below the scale M_{SUSY} are used. (5) In the relic density calculation, all slepton neutralino co-annihilation effects are included with an analysis valid for large $\tan\beta$. There are now several groups that have carried out this calculation^{13, 14, 15)}, and we have checked that they are generally in good agreement.

We have not assumed any specific GUT group relations, such as Yukawa unification or proton decay constraints (except for grand unification of the gauge coupling constants). Such relations depend on physics beyond the GUT scale about which little is known, and need not, for example, hold in string models, even when coupling constant unification is required.

3 mSUGRA Model

The mSUGRA model⁷⁾ is the simplest possible model with universal soft breaking masses at M_G . It depends on four parameters and one sign: m_0 , the masses of the scalar particles at M_G ; $m_{1/2}$, the gaugino masses at M_G ; A_0 , the cubic soft breaking mass at M_G ; $\tan\beta$, the ratio of the Higgs VEVs, $\langle H_2 \rangle / \langle H_1 \rangle$, at the electroweak scale; and the sign of μ , the Higgs mixing parameter in the superpotential ($W_\mu = \mu H_1 H_2$). We allow the above parameters to vary over the following ranges: $0 < m_0, m_{1/2} \leq 1$ TeV, $2 \leq \tan\beta \leq 45$, $|A_0| \leq 4m_{1/2}$.

It has been known from the beginning ^{8, 9)} that a_μ^{SUGRA} increases with $\tan\beta$. The leading terms come from the chargino ($\tilde{\chi}_1^\pm$) diagrams where the muon can polarize into a chargino and a sneutrino. Expanding for $(\mu \pm \tilde{m}_2)^2 \gg M_W^2$ (which generally is the case for mSUGRA), one finds for this leading term ¹⁶⁾,

$$a_\mu^{\text{SUGRA}} \cong \frac{\alpha}{4\pi} \frac{1}{\sin^2 \theta_W} \left(\frac{m_\mu^2}{m_{\tilde{\chi}_1^\pm} \mu} \right) \frac{\tan\beta}{1 - \frac{\tilde{m}_2^2}{\mu^2}} \left[1 - \frac{M_W^2}{\mu^2} \frac{1 + 3\frac{\tilde{m}_2^2}{\mu^2}}{\left(1 - \frac{\tilde{m}_2^2}{\mu^2}\right)^2} \right] F(x) \quad (8)$$

where $m_{\tilde{\chi}_1^\pm} \cong \tilde{m}_2 \cong 0.8m_{1/2}$, $x = m_\nu^2/m_{\tilde{\chi}_1^\pm}^2$ and $F(x)$ is a form factor arising from the loop integration. This implies that the sign of a_μ^{SUGRA} is determined by the sign of μ ¹⁷⁾, and since experimentally, Eq. (2), one has that a_μ has a positive anomaly, one has that

$$\mu > 0 \quad (9)$$

This result has immediate consequences for dark matter detection. Thus the scattering of neutralinos by nuclei in dark matter detectors is governed by the cross section $\sigma_{\tilde{\chi}_1^0-p}$, and for $\mu < 0$, cancellations can occur reducing these cross sections to below 10^{-12} pb in large regions of the parameter space ^{18, 19)}. This is exhibited in Fig. 1. If μ were negative, one would require a detector well beyond anything that is currently planned, and so dark matter experiments would not be able to scan the full SUSY parameter space. However, with Eq. 9, one finds that cross sections generally are greater than 10^{-10} ¹⁹⁾, accessible to future planned detectors such as GENIUS ²⁰⁾ or Cryoarray ²¹⁾.

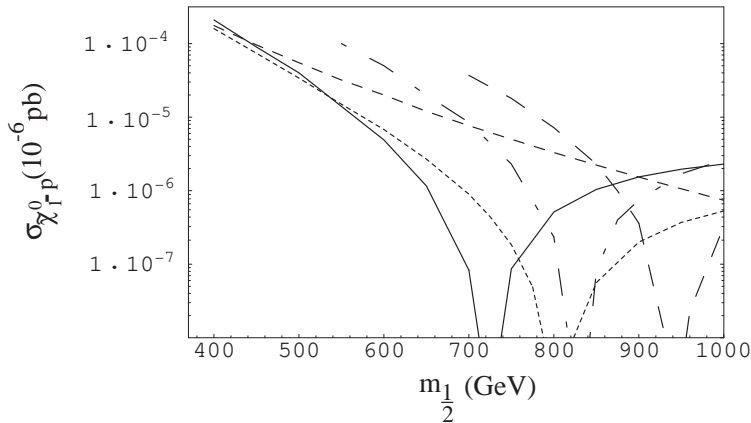


Figure 1: $\sigma_{\tilde{\chi}_1^0-p}$ for $\mu < 0$, $A_0 = 1500$ GeV, for $\tan\beta = 6$ (short dash), $\tan\beta = 8$ (dotted), $\tan\beta = 10$ (solid), $\tan\beta = 20$ (dot-dash), $\tan\beta = 25$ (dashed) ¹⁹⁾.

Eq. (9) also has important theoretical consequences for the mSUGRA model. Thus we first note that the combined experimental constraints on the Higgs mass and the $b \rightarrow s\gamma$ branching ratio, implies that most of the allowed parameter space is in the co-annihilation region of the parameter space, i. e. $m_{1/2} \gtrsim 300$ GeV. This means that m_0 is essentially determined in terms of $m_{1/2}$ (for fixed A_0 and $\tan\beta$) as can be seen in Fig. 2. In particular, this means that m_0 is an increasing function of $m_{1/2}$. Now a_μ^{SUGRA} decreases with increasing $m_{1/2}$ and increasing m_0 . Thus the lower bound of a_μ^{SUGRA} of Eq. (7) then implies an upper bound on $m_{1/2}$ (since an increase in $m_{1/2}$ cannot be compensated by a decrease of m_0). Thus the combined effects of the data is to give now both lower bounds on $m_{1/2}$ (from m_h and $b \rightarrow s\gamma$) and upper bounds on $m_{1/2}$ (from a_μ), as illustrated in Fig. 3. If however, the a_μ data had required $\mu < 0$ (instead of Eq. (9)) with the same lower bound on $|a_\mu^{\text{SUGRA}}|$, then the m_h and $b \rightarrow s\gamma$ constraints for this sign of μ would have essentially eliminated all the mSUGRA parameter space. Thus Eq. (7) also represents an experimental test of the validity of the mSUGRA model.

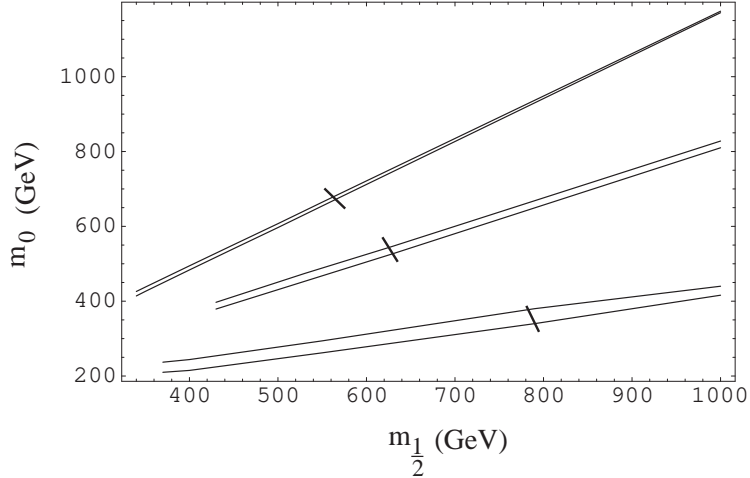


Figure 2: Corridors in the $m_0 - m_{1/2}$ plane allowed by the relic density constraint for $\tan\beta = 40$, $m_h > 111$ GeV, $\mu > 0$ for $A_0 = 0, -2m_{1/2}, 4m_{1/2}$ from bottom to top. The curves terminate at low $m_{1/2}$ due to the $b \rightarrow s\gamma$ constraint except for the $A_0 = 4m_{1/2}$ which terminates due to the m_h constraint. The short lines through the allowed corridors represent the high $m_{1/2}$ termination due to the lower bound on a_μ of Eq. (7). 16)

Since m_h is an increasing function of $m_{1/2}$ and $\tan\beta$, the fact that $m_{1/2}$ is bounded from above, and m_h is bounded from below implies a lower bound on

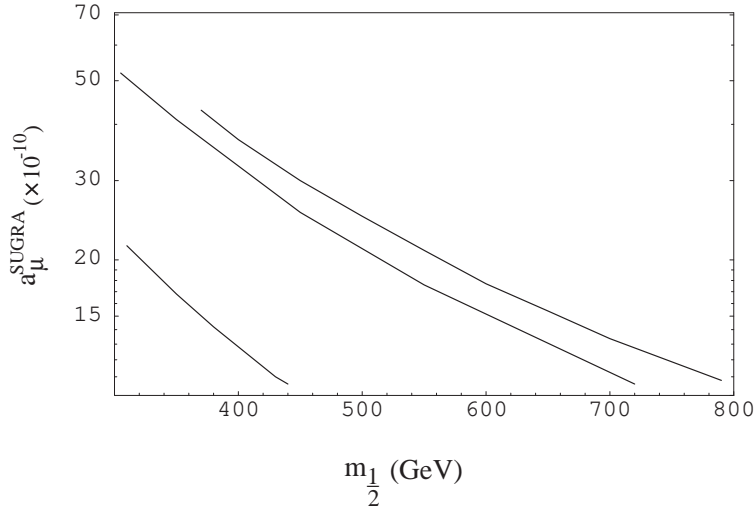


Figure 3: *mSUGRA* contribution to a_μ as a function of $m_{1/2}$ for $A_0 = 0$, $\mu > 0$, for $\tan\beta = 10, 30$ and 40 (bottom to top). 16)

$\tan\beta$. We find at the 95% C. L. that for $m_h > 114$ GeV

$$\tan\beta > 7(5) \quad \text{for} \quad A_0 = 0(-4m_{1/2}) \quad (10)$$

and for $m_h > 120$ GeV one would have

$$\tan\beta > 15(10) \quad \text{for} \quad A_0 = 0(-4m_{1/2}) \quad (11)$$

We see that the a_μ anomaly favors large $\tan\beta$. Fig. 3 also shows that the mSUGRA model cannot accommodate large values of a_μ^{SUGRA} , and if the final E821 results were significantly higher than 50×10^{-10} , this would be a signal for non-universal soft breaking.

The strong constraints on $m_{1/2}$ discussed above also sharpens considerably the predictions that mSUGRA has for the SUSY mass spectrum expected at accelerators. To see what these are, we consider the 90% C. L. on the a_μ anomaly, i.e. we require now $a_\mu^{\text{SUGRA}} > 20 \times 10^{-10}$ 22). In this case one finds that for $A_0 = 0$ that $\tan\beta > 10$. Then for $\tan\beta < 40$, $m_{1/2}$ and m_0 are constrained as follows:

$$m_{1/2} = (190 - 550) \text{ GeV}; \quad m_0 = (70 - 300) \text{ GeV} \quad (12)$$

In Table 1 we give the range expected for the SUSY masses implied by these constraints. All the masses except the light stop, \tilde{t}_1 , are insensitive to A_0 and the lower bound for $m_{\tilde{t}_1}$ can be lowered to 240 GeV by decreasing A_0 to $-4m_{1/2}$.

From this we see that the trilepton signal unfortunately would be out of reach of the Tevatron RUN II ($\tan \beta$ and $m_{1/2}$ are too large ²³) and RUN II (with 30 fb^{-1}) would only be able to see the light Higgs provided $m_h < 130 \text{ GeV}$ ²⁴. A 500 GeV NLC would be able to detect the h , $\tilde{\tau}_1$, and cover only part of the parameter space for the light selectron, \tilde{e}_1 . The LHC, however, would be able to see the full SUSY spectrum.

Table 1. Allowed ranges for SUSY masses in GeV for $mSUGRA$ assuming 90% C. L. for a_μ for $A_0 = 0$. The lower value of $m_{\tilde{\tau}_1}$ can be reduced to 240 GeV by changing A_0 to $-4m_{1/2}$. The other masses are not sensitive to A_0 . ¹⁶

$\tilde{\chi}_1^0$	$\tilde{\chi}_1^\pm$	\tilde{g}	$\tilde{\tau}_1$	\tilde{e}_1	\tilde{u}_1	\tilde{t}_1
(123-237)	(230-451)	(740-1350)	(134-264)	(145-366)	(660-1220)	(500-940)

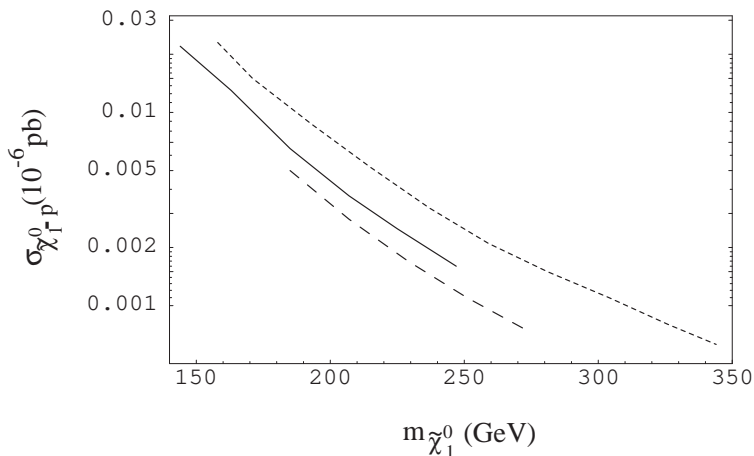


Figure 4: $\sigma_{\tilde{\chi}_1^0-p}$ as a function of the neutralino mass $m_{\tilde{\chi}_1^0}$ for $\tan \beta = 40$, $\mu > 0$ for $A_0 = -2m_{1/2}, 4m_{1/2}, 0$ from bottom to top. The curves terminate at small $m_{\tilde{\chi}_1^0}$ due to the $b \rightarrow s\gamma$ constraint for $A_0 = 0$ and $-2m_{1/2}$ and due to the Higgs mass bound ($m_h > 114 \text{ GeV}$) for $A_0 = 4m_{1/2}$. The curves terminate at large $m_{\tilde{\chi}_1^0}$ due to the lower bound on a_μ of Eq. (7). ¹⁶

We saw above that the experimental requirement that a_μ^{SUGRA} be positive, i. e. that $\mu > 0$, eliminated much of the parameter space that would not be accessible to dark matter detectors. In addition, the lower bound of Eq. (7) produces an upper bound on $m_{1/2}$ and m_0 , and since the dark matter detection cross section, $\sigma_{\tilde{\chi}_1^0-p}$, decreases with increasing m_0 and $m_{1/2}$, the lower bound on $\sigma_{\tilde{\chi}_1^0-p}$ is raised for the

remaining $\mu > 0$ part of the parameter space. Fig. 4 shows the expected cross sections for $\tan\beta = 40$, $\mu > 0$, $m_h > 114$ GeV, for $A_0 = -2m_{1/2}, 4m_{1/2}, 0$ (bottom to top). We see that there is a significant dependence on A_0 , and over the full range, $\sigma_{\tilde{\chi}_1^0-p} > 6 \times 10^{-10}$ pb. If the Higgs bound was raised to $m_h > 120$ GeV, then the lower bounds on $m_{1/2}$ increase to 200 GeV, 215 GeV, and 246 GeV respectively, significantly further reducing the parameter space.

If we reduce $\tan\beta$ one would expect $\sigma_{\tilde{\chi}_1^0-p}$ to fall. However, for lower $\tan\beta$, the upper bound on $m_{1/2}$ becomes more constraining, eliminating more of the high $m_{1/2}, m_0$ region, and thus compensating partially for the reduction of $\tan\beta$. This is seen in Fig. 5 where $\sigma_{\tilde{\chi}_1^0-p}$ is given for $\tan\beta = 10$, $A_0 = 0$ (upper curve) and $A_0 = -4m_{1/2}$ (lower curve). We have now that $\sigma_{\tilde{\chi}_1^0-p} > 4 \times 10^{-10}$ pb. Thus almost all the parameter space should now be accessible to future planned detectors such as GENIUS and Cryoarray.

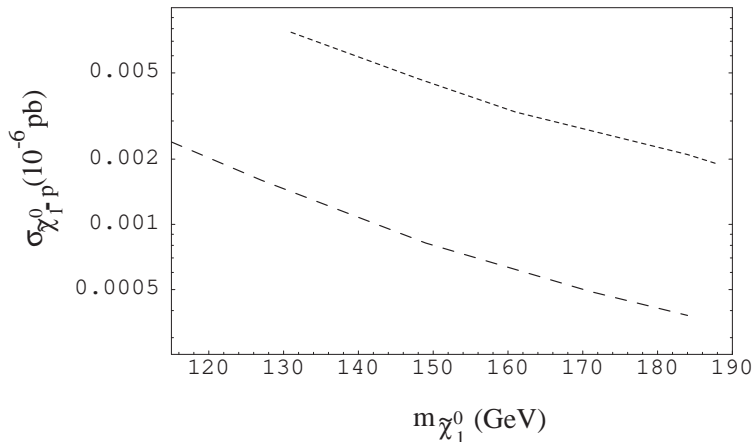


Figure 5: $\sigma_{\tilde{\chi}_1^0-p}$ as a function of $m_{\tilde{\chi}_1^0}$ for $\tan\beta = 10$, $\mu > 0$, $m_h > 114$ GeV for $A_0 = 0$ (upper curve), $A_0 = -4m_{1/2}$ (lower curve). The termination at low $m_{\tilde{\chi}_1^0}$ is due to the m_h bound for $A_0 = 0$, and the $b \rightarrow s\gamma$ bound for $A_0 = -4m_{1/2}$. The termination at high $m_{\tilde{\chi}_1^0}$ is due to the lower bound on a_μ of Eq. (7). ¹⁶⁾

4 Non-Universal Models

We consider here the case where there is non-universal soft breaking masses at M_G for the Higgs bosons and the third generation of squarks and sleptons. This possibility produces interesting new effects. One may parameterize the masses in

the following way:

$$\begin{aligned}
m_{H_1}^2 &= m_0^2(1 + \delta_1); & m_{H_2}^2 &= m_0^2(1 + \delta_2); \\
m_{q_L}^2 &= m_0^2(1 + \delta_3); & m_{t_R}^2 &= m_0^2(1 + \delta_4); & m_{\tau_R}^2 &= m_0^2(1 + \delta_5); \\
m_{b_R}^2 &= m_0^2(1 + \delta_6); & m_{l_L}^2 &= m_0^2(1 + \delta_7).
\end{aligned} \tag{13}$$

where m_0 is the universal soft breaking mass for the first two generations, $q_L = (\tilde{t}_L, \tilde{b}_L)$, $l_L = (\tilde{\nu}_L, \tilde{\tau}_L)$, and we assume that $-1 < \delta_i < +1$.

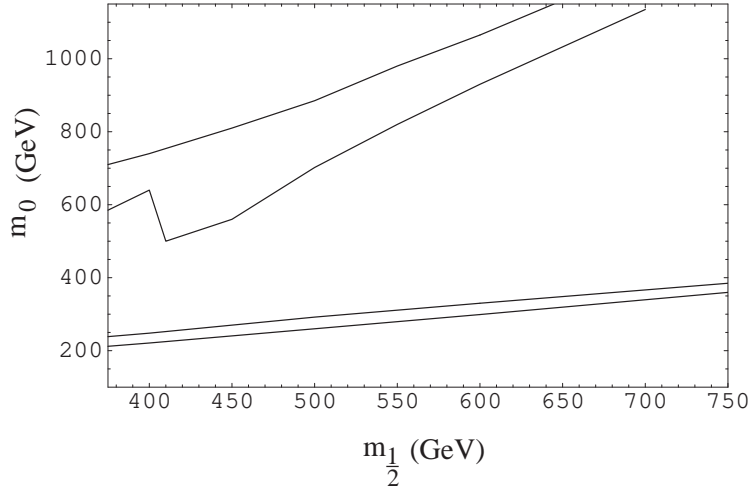


Figure 6: *Effect of a non-universal Higgs soft breaking mass enhancing the Z^0 s -channel pole contribution in the early universe annihilation, for the case of $\delta_2 = 1$, $\tan \beta = 40$, $A_0 = m_{1/2}$, $\mu > 0$. The lower band is the usual $\tilde{\tau}_1$ coannihilation region. The upper band is an additional region satisfying the relic density constraint arising from increased annihilation via the Z^0 pole due to the decrease in μ^2 increasing the higgsino content of the neutralino.* 19)

While this model has a number of additional parameters, one can understand the physics of what is implied from the following considerations. Electroweak symmetry breaking is governed by the μ parameter at the electroweak scale, and for low and intermediate $\tan \beta$ one has

$$\begin{aligned}
\mu^2 &= \frac{t^2}{t^2 - 1} \left[\left(\frac{1 - 3D_0}{2} + \frac{1}{t^2} \right) + \frac{1 - D_0}{2} (\delta_3 + \delta_4) \right. \\
&\quad \left. - \frac{1 + D_0}{2} \delta_2 + \frac{\delta_1}{t^2} \right] m_0^2 + \text{universal parts} + \text{loop corrections}.
\end{aligned} \tag{14}$$

Here $t = \tan \beta$, and $D_0 \cong 1 - (m_t/200 \text{ GeV} \sin \beta)^2 \cong 0.25$. (D_0 arises from running the RGE from M_G to the electroweak scale.) One sees that for $\tan \beta > 3$, the

universal part of μ^2 depending on m_0^2 is quite small, and so this term is sensitive to the amount of non-universal soft breaking that might be present. Now much of the physics is governed by μ^2 . If μ^2 is decreased, then the higgsino part of $\tilde{\chi}_1^0$ will increase. This has several effects. First it increases the $\tilde{\chi}_1^0 - \tilde{\chi}_1^0 - Z$ coupling which allows then the opening of a new neutralino annihilation channel through an s-channel Z pole, in the relic density calculation. This allows a new region of allowed relic density at high $\tan\beta$ and high m_0 . Second, since $\sigma_{\tilde{\chi}_1^0-p}$ depends on the interference term between the higgsino and gaugino parts of the neutralino, the dark matter detection cross section will be increased with increasing higgsino content. To illustrate these effects, we consider two cases

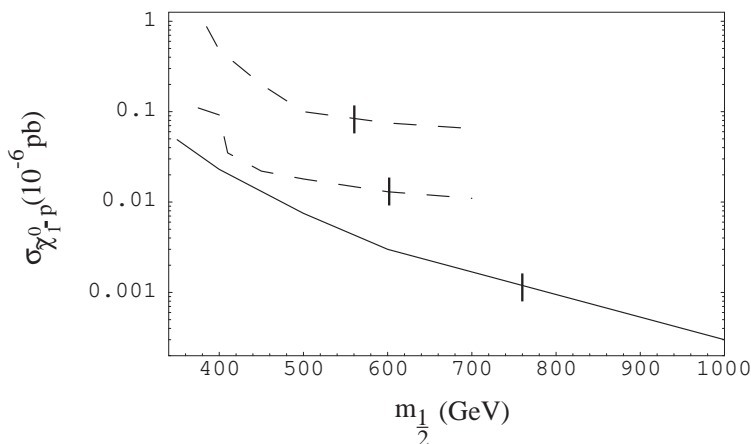


Figure 7: $\sigma_{\tilde{\chi}_1^0-p}$ as a function of $m_{1/2}$ ($m_{\tilde{\chi}_1^0} \cong 0.4m_{1/2}$) for $\tan\beta = 40$, $\mu > 0$, $m_h > 114$ GeV, $A_0 = m_{1/2}$ for $\delta_2 = 1$. The lower curve is for the $\tilde{\tau}_1 - \tilde{\chi}_1^0$ co-annihilation channel, and the dashed band is for the Z s-channel annihilation allowed by non-universal soft breaking. The curves terminate at low $m_{1/2}$ due to the $b \rightarrow s\gamma$ constraint. The vertical lines show the termination at high $m_{1/2}$ due to the lower bound on a_μ of Eq. (7). 16)

$$(1) \delta_2 = 1, \delta_i = 0, i \neq 2.$$

Here one sees that the m_0^2 term contributes negatively to μ^2 . The effect of this is shown in Fig. 6 where the region allowed by the relic density constraint in the $m_0 - m_{1/2}$ plane for $\tan\beta = 40$, $A_0 = m_{1/2}$ is given. The lower corridor, coming from the stau-neutralino co-annihilation is much the same as the $A_0 = 0$ corridor in Fig. 2. The upper channel, at higher m_0 , is due to the s-channel Z -pole annihilation. Fig. 7 shows the neutralino proton cross sections for corresponding allowed regions as a function of $m_{1/2}$ ($m_{\tilde{\chi}_1^0} \cong 0.4m_{1/2}$), for $\tan\beta = 40$. In spite of the fact that m_0 is quite high for the Z s-channel corridor, the cross sections is quite

large, and at least part of this region should be accessible to GENIUS -TF, and CDMS in the Soudan mine. This increase is due to the fact that the non-universality has lowered μ^2 .

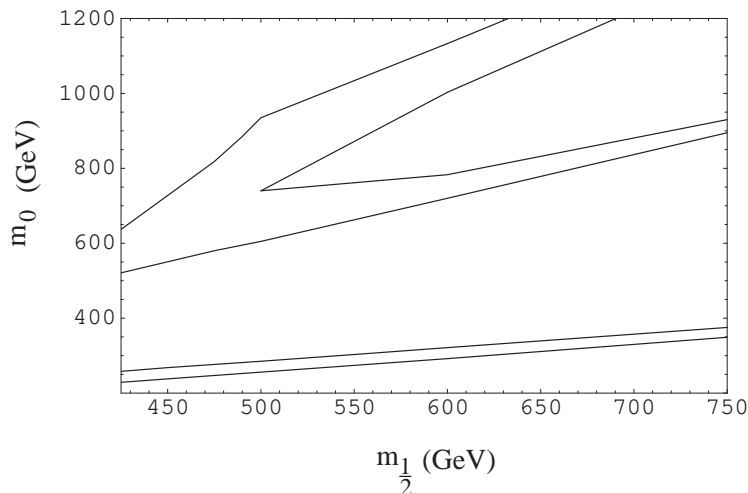


Figure 8: Allowed regions in the $m_0 - m_{1/2}$ plane for the case $\tan \beta = 40$, $A_0 = m_{1/2}$, $\mu > 0$. The bottom curve is the mSUGRA $\tilde{\tau}_1$ coannihilation band of Fig. 2 (shown for reference). The middle band is the actual $\tilde{\tau}_1$ coannihilation band when $\delta_{10} = -0.7$. The top band is an additional allowed region due to the enhancement of the Z^0 s-channel annihilation arising from the nonuniversality lowering the value of μ^2 and hence raising the higgsino content of the neutralino. For $m_{1/2} \lesssim 500$ GeV, the two bands overlap. ¹⁹⁾

$$(2) \delta_{10} (= \delta_3 = \delta_4 = \delta_5) = -0.7.$$

This is a model that might arise in a $SU(5)$ GUT, where only the particles of the $\overline{\mathbf{10}}$ representation in the third generation have non-universal soft breaking masses. Again, the non-universality lowers the value of μ^2 , allowing for a Z s-channel corridor in the relic density analysis. In addition, because the soft breaking mass of the stau is reduced, the co-annihilation channel occurs at a higher value of m_0 . This is shown in Fig. 8, for $\tan \beta = 40$, where the bottom band, the usual mSUGRA co-annihilation channel, is now moved up to much higher m_0 . (This co-annihilation and the Z -channel annihilation corridors merge for $m_{1/2} \lesssim 500$ GeV.) The corresponding cross sections are shown in Fig. 9. Again part of this parameter space should be accessible to the next round of dark matter detectors.

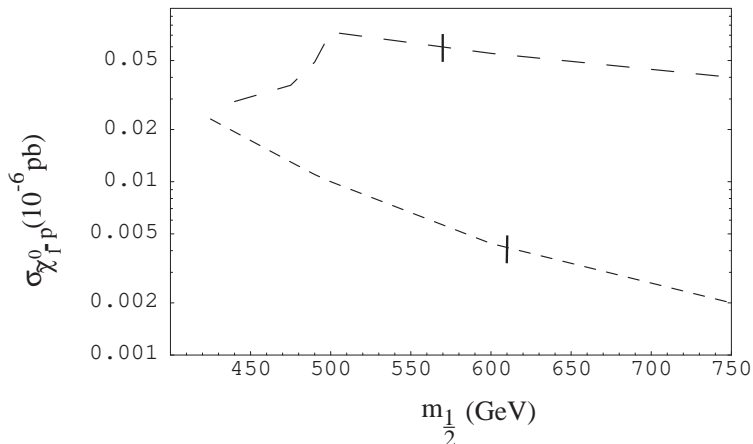


Figure 9: $\sigma_{\tilde{\chi}_1^0-p}$ as a function of $m_{1/2}$ for $\tan\beta = 40$, $\mu > 0$, $A_0 = m_{1/2}$ and $m_h > 114$ GeV. The lower curve is for the bottom of the $\tilde{\tau}_1 - \tilde{\chi}_1^0$ co-annihilation corridor, and the upper curve is for the top of the Z channel band. The termination at low $m_{1/2}$ is due to the $b \rightarrow s\gamma$ constraint, and the vertical lines are the upper bound on $m_{1/2}$ due to the lower bound of a_μ of Eq. (7). ¹⁶⁾

5 Conclusions

We have examined here the 2.6σ deviation of $a_\mu = (g_\mu - 2)/2$ from its predicted Standard Model result under the assumption that the effect is real and can be understood in terms supergravity GUT models with R-parity invariance. For mSUGRA models, the combined constraints from the a_μ , m_h , and the $b \rightarrow s\gamma$ decay constraints and the relic density of $\tilde{\chi}_1^0$ dark matter greatly limit the SUSY parameter space, greatly tightening the predictions the theory can make. The lower bound on a_μ produces an upper bound on $m_{1/2}$, and then the m_h and $b \rightarrow s\gamma$ constraints produce lower bounds on $m_{1/2}$ and $\tan\beta$. We find that for $m_h > 114$ GeV, that $\tan\beta > 7(5)$ for $A_0 = 0(-4m_{1/2})$ and for $m_h > 120$ GeV, $\tan\beta > 15(10)$ for $A_0 = 0(-4m_{1/2})$. The lower bound on $m_{1/2}$ pushes most of the parameter space into the co-annihilation domain effectively determining m_0 in terms of $m_{1/2}$. However, there is still a significant dependence on A_0 and $\tan\beta$.

The restrictions on the allowed range of $m_{1/2}$ and m_0 allow one now to make significant predictions concerning accelerator reaches for the SUSY particles. Thus we find at 90% C. L. bounds on a_μ that the Tevatron Run II should be able to see the light Higgs (if $m_h < 130$ GeV), but no other parts of the SUSY spectrum. A 500 GeV NLC should be able to see the h and $\tilde{\tau}_1$, and scan part of the parameter space where the \tilde{e}_1 is expected. The LHC should be able to detect the full SUSY

spectrum. Further, future planned dark matter detectors, GENIUS and Cryoarray, should be able to sample almost all of the SUSY parameter space. For other analyses within the mSUGRA framework see ²⁵⁾.

Non-universal SUGRA models can allow new regions in parameter space to open due to possible annihilation in the early universe through s-channel Z poles. For these types of non-universalities, which lower the value of μ^2 , the neutralino proton cross sections become larger, and part of these effects can possibly be tested with current detectors. Since non-universalities are phenomena determined by post-GUT physics, the dark matter detectors could allow one to learn about physics beyond the GUT scale.

The current anomaly in a_μ is a 2.6σ effect. However, the additional data that now exists, and the expected reduction of the theoretical errors should allow a determination in the near future of whether the effect is real.

6 Acknowledgements

This work was supported in part by National Science Foundation grant No. PHY-0070964.

References

1. H.N. Brown et.al., Muon (g-2) Collaboration, Phys. Rev. Lett. **86**, 2227 (2001).
2. I. Logashenko, Talk given at SUSY 2001, Dubna, Russia, June 2001.
3. W.J. Marciano, B.L. Roberts, hep-ph/0105056; S. Narison, hep-ph/0103199.
4. K. Melnikov, hep-ph/0105267.
5. P. Fayet, in Unification of the Fundamental Particle Interactions, edited by S. Ferrara, J. Ellis, and P. van Nieuwenhuizen (Plenum, New York, 1980); J. A. Grifols and A. Mendez, Phys. Rev. D **26**, 1809 (1982); J. Ellis, J. Hagelin and D.V. Nanopoulos, Phys. Lett. B **116**, 283 (1982); R. Barbieri and L. Maiani, Phys. Lett. B **117**, 203 (1982).
6. S. Ferrara and E. Remiddi, Phys. Lett. B **53**, 347 (1974).
7. A.H. Chamseddine, R. Arnowitt and P. Nath, Phys. Rev. Lett. **49**, 970 (1982); R. Barbieri, S. Ferrara and C.A. Savoy, Phys. Lett. B **119**, 343 (1982); L. Hall, J. Lykken and S. Weinberg, Phys. Rev. D **27**, 2359 (1983); P. Nath, R. Arnowitt and A.H. Chamseddine, Nucl. Phys. B **227**, 121 (1983).

8. D.A. Kosower, L.M. Krauss and N. Sakai, Phys. Lett. B **133**, 305 (1983).
9. T.C. Yuan, R. Arnowitt, A.H. Chamseddine and P. Nath, Z. Phys. C **26**, 407 (1984).
10. P. Igo-Kemenes, LEPC meeting, November 3, 2000 (<http://lephiggs.web.cern.ch/LEPHIGGS/talks/index.html>).
11. H. Haber, R. Hempfling, A.H. Hoang, Z. Phys. C **75**, 539 (1997).
12. G. Degrassi, P. Gambino and G. Giudice, JHEP **0012**, 009 (2000); M. Carena, D. Garcia, U. Nierste and C. Wagner, Phys. Lett. B **499**, 141 (2001).
13. R. Arnowitt, B. Dutta, Y. Santoso, hep-ph/0010244; hep-ph/0101020; Nucl. Phys. B **606**, 59 (2001).
14. J. Ellis, T. Falk, G. Gani, K. Olive and M. Srednicki, hep-ph/0102098; J. Ellis, T. Falk, K. Olive, Phys. Lett. B **444**, 367 (1998); J. Ellis, T. Falk, K. Olive, M. Srednicki, Astropart. Phys. **13**, 181 (2000); Erratum-ibid.**15**, 413 (2001).
15. M. Gomez, J. Vergados, hep-ph/0012020; M. Gomez, G. Lazarides, C. Pallis, Phys. Rev. D **61**, 123512 (2000); Phys. Lett. **B487**, 313 (2000).
16. R. Arnowitt, B. Dutta, B. Hu, Y. Santoso, Phys. Lett. B **505**, 177 (2001).
17. J.L. Lopez, D.V. Nanopoulos and X. Wang, Phys. Rev. D **49**, 366 (1994); U. Chattopadhyay and P. Nath, Phys. Rev. D **53**, 1648 (1996).
18. J. Ellis, A. Ferstl and K.A. Olive, Phys. Lett. B **481**, 304 (2000); Phys. Rev. D **63**, 065016 (2001).
19. R. Arnowitt, B. Dutta, Y. Santoso, Nucl. Phys. B **606**, 59 (2001).
20. H.V. Klapdor-Kleingrothaus *et al*, hep-ph/0103082.
21. R.J. Gaitskell, astro-ph/0106200.
22. A. Czarnecki, W.J. Marciano, Phys. Rev. D **64**, 013014 (2001).
23. V. Barger and C. Kao, Phys. Rev. D **60**, 115015 (1999); E. Accomando, R. Arnowitt and B. Dutta, Phys. Lett. B **475**, 176 (2000).
24. M. Carena *et al*, Report of the Tevatron Higgs Working Group, hep-ph/0010338.

25. J. Feng and K. Matchev, Phys. Rev. Lett. **86**, 3480 (2001); U. Chattopadhyay and P. Nath, hep-ph/0102157; S. Komine, T. Moroi and M. Yamaguchi, Phys. Lett. B **506**, 93 (2001); Phys. Lett. B **507**, 224 (2001); T. Ibrahim, U. Chattopadhyay and P. Nath, hep-ph/0102324; J. Ellis, D.V. Nanopoulos and K. A. Olive, hep-ph/0102331; S. Martin and J. Wells, hep-ph/0103067; H. Baer, C. Balazs, J. Ferrandis and X. Tata, hep-ph/0103280; F. Richard, hep-ph/0104106; D. Carvalho, J. Ellis, M. Gomez and S. Lola, hep-ph/0103256; S. Baek, T. Goto, Y. Okada and K. Okumura, hep-ph/0104146; Y. Kim and M. Nojiri, hep-ph/0104258; K. Choi, K. Hwang, S.K. Kang, K.Y. Lee and W.Y. Song, hep-ph/0103048; W. de Boer, M. Huber, C. Sander, D.I. Kazakov, hep-ph/0106311.